Article

DNA as Supramolecular Scaffold for Porphyrin Arrays on the Nanometer Scale

Leslie-Anne Fendt, Imenne Bouamaied, Sandra Thni, Nicolas Amiot, and Eugen Stulz

J. Am. Chem. Soc., **2007**, 129 (49), 15319-15329 • DOI: 10.1021/ja075711c

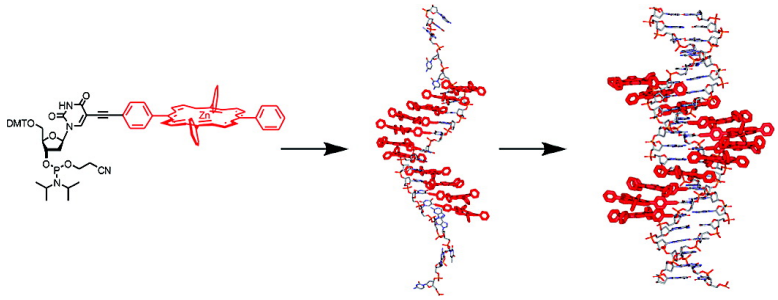

More About This Article

Additional resources and features associated with this article are available within the HTML version:

- Supporting Information
- Access to high resolution figures
- Links to articles and content related to this article
- Copyright permission to reproduce figures and/or text from this article

View the Full Text HTML

J|A|C|S
ARTICLES
Published on Web 11/16/2007

DNA as Supramolecular Scaffold for Porphyrin Arrays on the Nanometer Scale

Leslie-Anne Fendt,[‡] Imenne Bouamaied,[†,‡] Sandra Thöni,[‡] Nicolas Amiot,[‡] and Eugen Stulz*[,†]

Contribution from the School of Chemistry, University of Southampton, Highfield, Southampton SO17 1BJ, U.K., and Department of Chemistry, University of Basel, St. Johanns-Ring 19, 4056 Basel, Switzerland

Received July 31, 2007; E-mail: est@soton.ac.uk

Abstract: Tetraphenyl porphyrin substituted deoxyuridine was used as a building block to create discrete multiporphyrin arrays *via* site specific incorporation into DNA. The successful covalent attachment of up to 11 tetraphenyl porphyrins in a row onto DNA shows that there is virtually no limitation in the amount of substituents, and the porphyrin arrays thus obtained reach the nanometer scale (~10 nm). The porphyrin substituents are located in the major groove of the dsDNA and destabilize the duplex by ΔT_m 5−7 °C per porphyrin modification. Force-field structure minimization shows that the porphyrins are either in-line with the groove in isolated modifications or aligned parallel to the nucleobases in adjacent modifications. The CD signals of the porphyrins are dominated by a negative peak arising from the intrinsic properties of the building block. In the single strands, the porphyrins induce stabilization of a secondary helical structure which is confined to the porphyrin modified part. This arrangement can be reproduced by force-field minimization and reveals an elongated helical arrangement compared to the double helix of the porphyrin−DNA. This secondary structure is disrupted above ~55 °C (T_p) which is shown by various melting experiments. Both absorption and emission spectroscopy disclose electronic interactions between the porphyrin units upon stacking along the outer rim of the DNA leading to a broadening of the absorbance and a quenching of the emission. The single-stranded and double-stranded form show different spectroscopic properties due to the different arrangement of the porphyrins. Above T_p the electronic properties (absorption and emission) of the porphyrins change compared to room temperature measurements due to the disruption of the porphyrin stacking at high temperature. The covalent attachment of porphyrins to DNA is therefore a suitable way of creating helical stacks of porphyrins on the nanometer scale.

1. Introduction

Porphyrins and their derivatives are currently of major interest in the construction of light-harvesting complexes,[1] in molecular photovoltaics[2,3] and in the design of new systems for optoelectronic devices.[2,4] To create functional supramolecular complexes,[5] both covalent connection[6] and coordination chemistry approaches[7] are being used. This approach allows combination of the porphyrins with a variety of other electronically active groups such as phthalocyanines, fullerenes, 3d transition metal

[†] University of Southampton.
[‡] University of Basel.

(1) (a) Furutsu, D.; Satake, A.; Kobuke, Y. *Inorg. Chem.* **2005**, *44* (13), 4460−4462. (b) Hwang, I. W., et al. *Chem.−Eur. J.* **2005**, *11* (12), 3753−3761. (c) Nakamura, Y.; Aratani, N.; Osuka, A. *Chem. Soc. Rev.* **2007**, *36*, (6), 831−845.
(2) Schmidt-Mende, L.; Campbell, W. M.; Wang, Q.; Jolley, K. W.; Officer, D. L.; Nazeeruddin, M. K.; Grätzel, M. *ChemPhysChem* **2005**, *6* (7), 1253−1258.
(3) (a) Imahori, H.; Fujimoto, A.; Kang, S.; Hotta, H.; Yoshida, K.; Umeyama, T.; Matano, Y.; Isoda, S. *Adv. Mater.* **2005**, *17* (14), 1727−1730. (b) Imahori, H. *J. Mater. Chem.* **2007**, *17*, (1), 31−41.
(4) Straight, S. D.; Andreasson, J.; Kodis, G.; Bandyopadhyay, S.; Mitchell, R. H.; Moore, T. A.; Moore, A. L.; Gust, D. *J. Am. Chem. Soc.* **2005**, *127*, (26), 9403−9409.
(5) Bouamaied, I.; Coskun, T.; Stulz, E. In *Structure & Bonding*; Alessio, E., Ed.; Springer: Heidelberg, 2006; Vol. 121, pp 1−48.
(6) Holten, D.; Bocian, D. F.; Lindsey, J. S. *Acc. Chem. Res.* **2002**, *35*, (1), 57−69. Kieran, A. L.; Pascu, S. I.; Jarrosson, T.; Gunter, M. J.; Sanders, J. K. M. *Chem. Commun.* **2005**, (14), 1842−1844. de la Torre, G.; Giacalone, F.; Segura, J. L.; Martin, N.; Guldi, D. M. *Chem.−Eur. J.* **2005**, *11*, (4), 1267−1280.
(7) (a) Michelsen, U.; Hunter, C. A. *Angew. Chem., Int. Ed.* **2000**, *39* (4), 764−767. (b) Stulz, E.; Scott, S. M.; Bond, A. D.; Teat, S. J.; Sanders, J. K. M. *Chem.−Eur. J.* **2003**, *9* (24), 6039−6048. (c) Iengo, E.; Zangrando, E.; Alessio, E.; Chambron, J. C.; Heitz, V.; Flamigni, L.; Sauvage, J. P. *Chem.−Eur. J.* **2003**, *9* (23), 5879−5887. (d) Flamingi, L.; Heitz, V.; Sauvage, J.-P. *Struct. Bonding* **2006**, *121*, 217−262; (e) Iengo, E.; Zangrando, E.; Alessio, E. *Acc. Chem. Res.* **2006**, *39* (11), 841−851. (f) Iengo, E.; Zangrando, E.; Alessio, E.; Chambron, J. C.; Heitz, V.; Flamigni, L.; Sauvage, J. P. *Chem.−Eur. J.* **2003**, *9*, (23), 5879−5887. (g) Iengo, E.; Zangrando, E.; Alessio, E. *Eur. J. Inorg. Chem.* **2003**, (13), 2371−2384. (h) Iengo, E.; Scandola, F.; Alessio, E. *Struct. Bonding*, **2006**, *121*, 105−144. (i) Prodi, A.; Chiorboli, C.; Scandola, F.; Iengo, E.; Alessio, E.; Dobrawa, R.; Wurthner, F. *J. Am. Chem. Soc.* **2005**, *127*, (5), 1454−1462. (j) Kumar, P. P.; Premaladha, G.; Maiya, B. G. *Chem. Commun.* **2005**, (30), 3823−3825. (k) Johnstone, K. D.; Yamaguchi, K.; Gunter, M. J. *Org. Biomol. Chem.* **2005**, *3*, (16), 3008−3017. (l) Gunter, M. J. *Struct. Bonding* **2006**, *121*, 263−295. (m) Terazono, Y.; Kodis, G.; Liddell, P. A.; Garg, V.; Gervaldo, M.; Moore, T. A.; Moore, A. L.; Gust, D. *Photochem. Photobiol.* **2007**, *83*, (2), 464−469. (n) Kieran, A. L.; Bond, A. D.; Belenguer, A. M.; Sanders, J. K. M. *Chem. Commun.* **2003**, *9* (21), 2674−2675. (o) Corbett, P. T.; Leclaire, J.; Vial, L.; West, K. R.; Wietor, J. L.; Sanders, J. K. M.; Otto, S. *Chem. Rev.* **2006**, *106* (9), 3652−3711. (p) Atefi, F.; McMurtrie, J. C.; Turner, P.; Duriska, M.; Arnold, D. P. *Inorg. Chem.* **2006**, *45* (16), 6479−6489. (q) Ercolani, G. *Struct. Bonding* **2006**, *121*, 167−215. (r) Fanti, C.; Monti, D.; La Monica, L.; Ceccacci, F.; Mancini, G.; Paolesse, R. *J. Porphyr. Phthalocyanines* **2003**, *7* (2), 112−119. (s) Kobuke, Y. *Struct. Bonding*, **2006**, *121*, 49−104. (t) Hupp, J. T. In *Struct. Bonding* **2006**, *121*, 145−166.

complexes, or dipyrrins. Very promising candidates to obtain electronic or photonic wires are linear multiporphyrin arrays, since these can efficiently transfer energy or electrons upon photoirradiation.[8] Here again, both covalent and noncovalent approaches were applied. Very important is the substitution pattern and the metalation state of the porphyrin,[9] and changing these parameters allows fine-tuning of the electronic interactions between the units which is vital in the design of electronic gradients for efficient energy or electron transfer.[10]

Despite the sophistication of these systems, the major disadvantage in their structure design is that it is generally not trivial to replace the building blocks in the array, e.g., a porphyrin by a bipy complex or another organic dye, and a complete redesign and resynthesis of the entire array may be necessary. Such a replacement might be necessary in order to fine-tune the electronic interactions between the individual units. It would therefore be convenient to have a general building block system, where the mode of connectivity is largely independent of the structure of the electronically active molecule to be incorporated into the array. Once again, nature provides us with the most advanced templates to overcome this problem. Recently DNA has become attractive as a supramolecular scaffold to produce nanoscaled entities and has gained increasing importance in nanobiotechnology,[11] e.g., to specifically connect nanoparticles, in DNA chip technology and nanolithography, to create nanomechanical devices or to construct protein arrays and nanowires.[12] The nucleobases themselves have been substituted to create a functional DNA,[13] and examples include the use of "locked" DNA (LNA) building blocks substituted with methoxy or piperazino groups[14] or metal complexes to form stable duplexes,[15] polyaldehyde modified DNA for the deposition of Ag(0),[16] direct attachment of fluorophores,[17,18] 3d transition metal complexes,[19] ferrocenes,[20] and pyrenes.[21] A high-density functionalized DNA (fDNA) from modified dNTPs using PCR was also achieved.[22] Replacing the nucleobase with salen or hydroxypyridone metal complexes,[23] methyl red dyes,[24] pyrenes[25] and phenyls, biphenyls, or bipyridyls[26] leads to stabilized DNA duplexes or discrete self-assembled metal arrays in an artificial DNA.[27] Recently, DNA has been used as a template to create photonic wires.[28]

In this respect, we are in the course of exploring the use of DNA to connect multiple porphyrins that are attached directly to the nucleobases through rigid acetylene spacers. We have previously shown that different porphyrins can be attached to thymidine *via* Sonogashira coupling between 5-iodo deoxyuridine and alkyne substituted porphyrins,[29] thus giving access to a variety of building blocks using a general synthetic route. These can be transformed into the corresponding phosphoramidites and used for standard solid-phase DNA synthesis using an automated synthesizer.[30] We have thus made tetranucleotides that act as a scaffold for diporphyrin arrays, which show efficient energy transfer between two different free base or zinc porphyrins in organic solvents such as chloroform.[31] These tetranucleotides did not form duplexes with the complementary tetraadenosine, presumably due to electrostatic repulsion which becomes a dominant factor in apolar solvents. However, the covalent internal modification of longer DNA strands with porphyrins according to this route and the subsequent analysis

(8) (a) Drain, C. M. *Proc. Natl. Acad. Sci. U.S.A.* **2002**, *99* (8), 5178−5182. (b) Koepf, M.; Trabolsi, A.; Elhabiri, M.; Wytko, J. A.; Paul, D.; Albrecht-Gary, A. M.; Weiss, J. *Org. Lett.* **2005**, *7*, (7), 1279−1282. (c) D'Souza, F.; Ito, O. *Coord. Chem. Rev.* **2005**, *249* (13−14), 1410−1422. (d) Schumacher, A. L.; Sandanayaka, A. S. D.; Hill, J. P.; Ariga, K.; Karr, P. A.; Araki, Y.; Ito, O.; D'Souza, F. *Chem.—Eur. J.* **2007**, *13* (16), 4628−4635.

(9) Kalyanasundaram, K. *Photochemistry of Polypyridine and Porphyrin Complexes*; Academic Press: London, 1992.

(10) (a) Flamigni, L.; Barigelletti, F.; Armaroli, N.; Collin, J. P.; Sauvage, J. P.; Williams, J. A. G. *Chem.—Eur. J.* **1998**, *4* (9), 1744−1754. (b) Dixon, I. M.; Collin, J. P.; Sauvage, J. P.; Barigelletti, F.; Flamigni, L. *Angew. Chem., Int. Ed.* **2000**, *39*, (7), 1292−1295. (c) Flamigni, L.; Dixon, I. M.; Collin, J. P.; Sauvage, J. P. *Chem. Commun.* **2000**, (24), 2479−2480; (d) Flamigni, L.; Marconi, G.; Dixon, I. M.; Collin, J. P.; Sauvage, J. P. *J. Phys. Chem. B* **2002**, *106*, (26), 6663−6671.

(11) (a) Wengel, J. *Org. Biomol. Chem.* **2004**, *2*, (3), 277−280. (b) Carell, T.; Behrens, C.; Gierlich, J. *Org. Biomol. Chem.* **2003**, *1*, (13), 2221−2228.

(12) (a) Mirkin, C. A. *Inorg. Chem.* **2000**, *39*, (11), 2258−2272; (b) Eckardt, L. H.; Naumann, K.; Matthias Pankau, W.; Rein, M.; Schweitzer, M.; Windhab, N.; von Kiedrowski, G. *Nature* **2002**, *420* (6913), 286. (c) Li, M.; Mann, S. *J. Mater. Chem.* **2004**, *14* (14), 2260−2263. (d) Li, Z.; Jin, R. C.; Mirkin, C. A.; Letsinger, R. L. *Nucleic Acids Res.* **2002**, *30* (7), 1558−1562. (e) Yan, H.; Park, S. H.; Finkelstein, G.; Reif, J. H.; LaBean, T. H. *Science* **2003**, *301* (5641), 1882−1884. (f) Shu, D.; Moll, W.-D.; Deng, Z.; Mao, C.; Guo, P. *Nano Lett.* **2004**, *4*, (9), 1717−1723. (g) Park, S.-J.; Lazarides, A. A.; Storhoff, J. J.; Pesce, L.; Mirkin, C. A. *J. Phys. Chem. B* **2004**, *108* (33), 12375−12380. (h) Nakao, H.; Shiigi, H.; Yamamoto, Y.; Tokonami, S.; Nagaoka, T.; Sugiyama, S.; Ohtani, T. *Nano Lett.* **2003**, *3*, (10), 1391−1394; (i) Benenson, Y.; Adar, R.; Paz-Elizur, T.; Livneh, Z.; Shapiro, E. *Proc. Natl. Acad. Sci. U.S.A.* **2003**, *100*, (5), 2191−2196. (j) Zhang, H.; Li, Z.; Mirkin, C. A. *Adv. Mater.* **2002**, *14*, (20), 1472−1274. (k) Seeman, N. C. *Chem. Biol.* **2003**, *10*, (12), 1151−1159. (l) Seeman, N. C. *Nature* **2003**, *421*, (6921), 427−431. (m) LaBean, T. *Nat. Mater.* **2006**, *5*, (10), 767−768.

(13) Kottysch, T.; Ahlborn, C.; Brotzel, F.; Richert, C. *Chem.—Eur. J.* **2004**, *10*, (16), 4017−4028.

(14) Raunkjaer, M.; Sorensen, M. D.; Wengel, J. *Org. Biomol. Chem.* **2005**, *3*, (1), 130−135.

(15) Kalek, M.; Madsen, A. S.; Wengel, J. *J. Am. Chem. Soc.* **2007**, *129*, (30), 9392−9400.

(16) Burley, G. A.; Gierlich, J.; Mofid, M. R.; Nir, H.; Tal, S.; Eichen, Y.; Carell, T. *J. Am. Chem. Soc.* **2006**, *128*, (5), 1398−1399.

(17) Ranasinghe, R. T.; Brown, T. *Chem. Commun.* **2005**, (44), 5487−5502.

(18) (a) Obayashi, T.; Masud, M. M.; Ozaki, A. N.; Ozaki, H.; Kuwahara, M.; Sawai, H. *Bioorg. Med. Chem. Lett.* **2002**, *12*, (8), 1167−1170. (b) Foldes-Papp, Z.; Angerer, B.; Thyberg, P.; Hinz, M.; Wennmalm, S.; Ankenbauer, W.; Seliger, H.; Holmgren, A.; Rigler, R. *J. Biotechnol.* **2001**, *86*, (3), 203−224; (c) Foldes-Papp, Z.; Angerer, B.; Ankenbauer, W.; Rigler, R. *J. Biotechnol.* **2001**, *86*, (3), 237−253. (d) Seela, F.; Feiling, E.; Gross, J.; Hillenkamp, F.; Ramzaeva, N.; Rosemeyer, H.; Zulauf, M. *J. Biotechnol.* **2001**, *86*, (3), 269−279; (e) Hurley, D. J.; Seaman, S. E.; Mazura, J. C.; Tor, Y. *Org. Lett.* **2002**, *4* (14), 2305−2308.

(19) (a) Hurley, D. J.; Tor, Y. *J. Am. Chem. Soc.* **2002**, *124* (14), 3749−3762. (b) Khan, S. I.; Beilstein, A. E.; Smith, G. D.; Sykora, M.; Grinstaff, M. W. *Inorg. Chem.* **1999**, *38*, (10), 2411−2415. (c) Khan, S. I.; Beilstein, A. E.; Grinstaff, M. W. *Inorg. Chem.* **1999**, *38* (3), 418−419.

(20) (a) Long, Y. T.; Li, C. Z.; Sutherland, T. C.; Chahma, M.; Lee, J. S.; Kraatz, H. B. *J. Am. Chem. Soc.* **2003**, *125* (29), 8724−8725. (b) Wlassoff, W. A.; King, G. C. *Nucleic Acids Res.* **2002**, *30* (12), 7.

(21) (a) Mayer-Enthart, E.; Wagenknecht, H.-A. *Angew. Chem.-Int. Ed.* **2006**, *45* (20), 3372−3375. (b) Barbaric, J.; Wagenknecht, H.-A. *Org. Biomol. Chem.* **2006**, *4* (11), 2088−2090. (c) Nakamura, M.; Shimomura, Y.; Ohtoshi, Y.; Sasa, K.; Hayashi, H.; Nakano, H.; Yamana, K. *Org. Biomol. Chem.* **2007**, *5* (12), 1945−1951.

(22) Jager, S.; Rasched, G.; Kornreich-Leshem, H.; Engeser, M.; Thum, O.; Famulok, M. *J. Am. Chem. Soc.* **2005**, *127*, (43), 15071−15082.

(23) Clever, G. H.; Polborn, K.; Carell, T. *Angew. Chem.-Int. Ed.* **2005**, *44*, (44), 7204−7208.

(24) Kashida, H.; Tanaka, M.; Baba, S.; Sakamoto, T.; Kawai, G.; Asanuma, H.; Komiyama, M. *Chem.—Eur. J.* **2006**, *12* (3), 777−784.

(25) Malinovskii, V. L.; Samain, F.; Häner, R. *Angew. Chem., Int. Ed.* **2007**, *46*, (24), 4464−4467.

(26) (a) Zahn, A.; Leumann, C. J. *Bioorg. Med. Chem.* **2006**, *14*, (18), 6174−6188. (b) Brotschi, C.; Mathis, G.; Leumann, C. J. *Chem.—Eur. J.* **2005**, *11* (6), 1911−1923. (c) Zahn, A.; Brotschi, C.; Leumann, C. J. *Chem.—Eur. J.* **2005**, *11* (7), 2125−2129. (d) Brotschi, C.; Leumann, C. J. *Nucleosides Nucleotides Nucleic Acids* **2003**, *22* (5−8), 1195−1197. (e) Brotschi, C.; Leumann, C. J. *Angew. Chem., Int. Ed.* **2003**, *42* (14) 1655−1658. (f) Brotschi, C.; Haberli, A.; Leumann, C. J. *Angew. Chem., Int. Ed.* **2001**, *40*, (16), 3012−3014. (g) Hunziker, J.; Mathis, G. *Chimia* **2005**, *59* (11), 780−784.

(27) Tanaka, K.; Tengeiji, A.; Kato, T.; Toyama, N.; Shionoya, M. **2003**, *299* (5610), 1212−1213.

(28) (a) Heilemann, M.; Kasper, R.; Tinnefeld, P.; Sauer, M. *J. Am. Chem. Soc.* **2006**, *128* (51), 16864−16875. (b) Sanchez-Mosteiro, G.; van Dijk, E.; Hernando, J.; Heilemann, M.; Tinnefeld, P.; Sauer, M.; Koberlin, F.; Patting, M.; Wahl, M.; Erdmann, R.; van Hulst, N. F.; Garcia-Parajo, M. F. *J. Phys. Chem. B* **2006**, *110*, (51), 26349−26353.

(29) Bouamaied, I.; Stulz, E. *Synlett* **2004**, (9), 1579−1583.

(30) Bouamaied, I.; Stulz, E. *Chimia* **2005**, *59*, (3), 101−104.

(31) Bouamaied, I.; Fendt, L.-A.; Wiesner, M.; Häussinger, D.; Amiot, N.; Thöni, S.; Stulz, E. *Pure Appl. Chem.* **2006**, *78* (11), 2003−2014.

Scheme 1. Sequences of the Porphyrin−DNA Strands and of the Complementary Strands

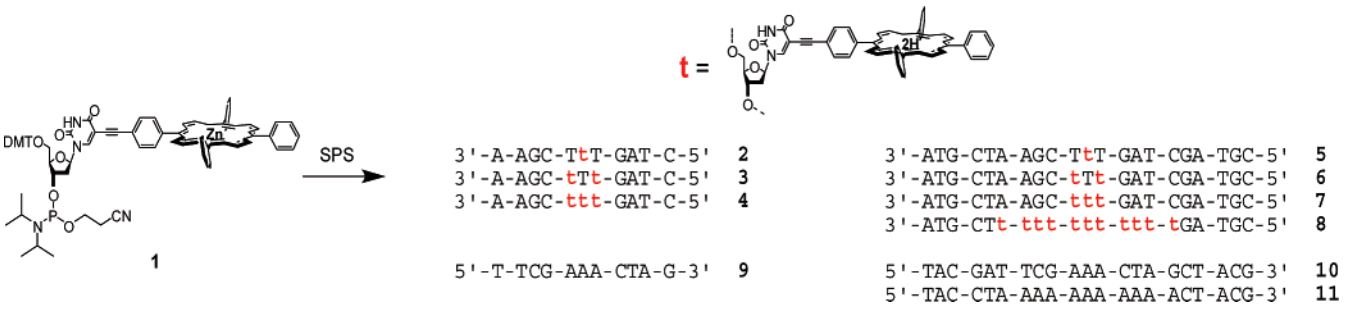

of the impact on structure and electronic properties in aqueous solutions have not been reported to date. In fact, nothing is known about DNA that is modified with more than one large and sterically demanding metal complex in a row. Upon hybridization with the complementary strand, the porphyrin units should be placed in a predetermined three-dimensional orientation, more precisely in the major groove of the double helix, giving access to new multiporphyrin arrays on the nanometer scale. So far, mainly noncovalent interactions of porphyrins with DNA, i.e., groove binding and intercalation,[32] single-porphyrin modifications,[33] or postsynthetically derivatized DNA strands[34] were studied. Porphyrins are also very useful as chiroptical probes for DNA structures.[35] Our system now offers a complementary template to peptidic arrays,[36] cellulose scaffolds,[37] and noncovalent helical assemblies.[38] Here, we describe the synthesis and analysis of DNA strands which are substituted to varying degrees of tetraphenyl porphyrins. This serves as proof of concept that multichromophore arrays can be created that are based on the porphyrin−nucleotide as a building block system and that the overall composition of the array can be tuned simply by reprogramming the input sequence in the DNA synthesizer.

2. Synthesis of the Porphyrin−DNA and Duplex Stability

In order to compare the stability of DNA duplexes with various amounts of porphyrin modifications, and also to study the influence of the length of the DNA on the electronic properties of the porphyrin, two different lengths of oligo deoxynucleotides (ODNs) were chosen. We synthesized 11-mer and 21-mer sequences as shown in Scheme 1. The tetraphenyl porphyrin (TPP) derivatized phosphoramidite building block dU^{ZnTPP} **1** was incorporated site specifically into ODNs **2**−**8** using solid phase automated DNA synthesis, where the coupling time for the modified building block was increased to 10 min. Due to the strongly acidic conditions during DNA synthesis (DMT deprotection with dichloro acetic acid), demetalation of the porphyrins is quantitative, and the arrays are obtained in the free-base form of the porphyrins. Purification of the porphyrin−DNA strands was achieved either by a combination of denaturing polyacrylamide gel electrophoresis (PAGE) and reversed-phase (RP) HPLC or by using fluorous affinity chromatography.[39] In the latter case, the 5′-terminal nucleotide contained a fluorous tagged DMT group. The purity was confirmed by both RP HPLC and MALDI-TOF MS (Table 1). The ODNs contain one central modification (**2**, **5**), two porphyrins separated by one thymidine (**3**, **6**), or three consecutive porphyrins (**4**, **7**). The successful incorporation of 11 porphyrins in a row into sequence **8** shows that there seems to be virtually no synthetic limitation to the amount of modifica-

Table 1. Analytical Data (MALDI-TOF MS) and Melting Temperatures (T_m) of ODNs **2** to **8** with the Corresponding Duplexes (see Scheme 1 for Sequences)[a]

	m/z (calcd)	T_m [°C]	ΔT_m/Por [°C]
2	3968.0 (3969.3)	**2•9** 30.4	6.5
3	4604.8 (4596.6)	**3•9** 23.5	6.7
4	5241.5 (5239.4)	**4•9** 16.4	6.8
5	7073.0 (7083.4)	**5•10** 57.1	6.4
6	7709.8 (7717.5)	**6•10** 53.7	4.9
7	8346.5 (8359.8)	**7•10** 50.1	4.5
8	13 393.6 (13 339.0)	**8•11** 21.2	3.1

[a] Thermal denaturation measurements were performed in 100 mM NaCl, 50 mM KH_2PO_4, pH 7.0, c(ODN) = 10^{-6} M.

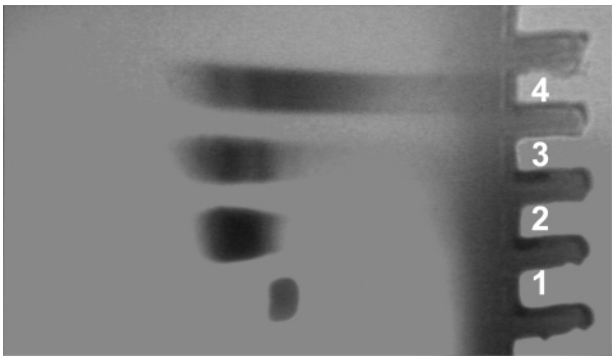

Figure 1. Denaturing PAGE of the 21-mer DNA strands visualized by UV illumination. Lane 1, unmodified DNA; lane 2, **5**; lane 3, **6**; lane 4, **7**.

(32) (a) Pasternack, R. F.; Gibbs, E. J.; Bruzewicz, D.; Stewart, D.; Shannon, K. *J. Am. Chem. Soc.* **2002**, *124* (14), 3533−3539. (b) Jain, R. K.; Sarracino, D. A.; Richert, C. *Chem. Commun.* **1998**, (3), 423−424. (c) McMillin, D. R.; McNett, K. M. *Chem. Rev.* **1998**, *98* (3), 1201−1219. (d) Marzilli, L. G.; Petho, G.; Lin, M. F.; Kim, M. S.; Dixon, D. W. *J. Am. Chem. Soc.* **1992**, *114* (19), 7575−7577.
(33) (a) Dubey, I.; Pratviel, G.; Meunier, B. *J. Chem. Soc., Perkin Trans. 1* **2000**, (18), 3088−3095. (b) Morales-Rojas, H.; Kool, E. T. *Org. Lett.* **2002**, *4* (25), 4377−4380.
(34) (a) Endo, M.; Shiroyama, T.; Fujitsuka, M.; Majima, T. *J. Org. Chem.* **2005**, *70* (19), 7468−7472. (b) Endo, M.; Seeman, N. C.; Majima, T. *Angew. Chem., Int. Ed.* **2005**, *44* (37), 6074−6077.
(35) (a) Balaz, M.; De Napoli, M.; Holmes, A. E.; Mammana, A.; Nakanishi, K.; Berova, N.; Purrello, R. *Angew. Chem., Int. Ed.* **2005**, *44* (26), 4006−4009. (b) Balaz, M.; Li, B. C.; Steinkruger, J. D.; Ellestad, G. A.; Nakanishi, K.; Berova, N. *Org. Biomol. Chem.* **2006**, *4* (10), 1865−1867.
(36) (a) Hasobe, T.; Kamat, P. V.; Troiani, V.; Solladie, N.; Ahn, T. K.; Kim, S. K.; Kim, D.; Kongkanand, A.; Kuwabata, S.; Fukuzumi, S. *J. Phys. Chem. B* **2005**, *109* (1), 19−23. (b) Dunetz, J. R.; Sandstrom, C.; Young, E. R.; Baker, P.; Van Name, S. A.; Cathopolous, T.; Fairman, R.; de Paula, J. C.; Akerfeldt, K. S. *Org. Lett.* **2005**, *7*, (13), 2559−2561.
(37) Redl, F. X.; Lutz, M.; Daub, J. *Chem.−Eur. J.* **2001**, *7*, (24), 5350−5358.
(38) (a) Mammana, A.; De Napoli, M.; Lauceri, R.; Purrello, R. *Bioorg. Med. Chem.* **2005**, *13* (17), 5159−5163. (b) Gulino, F. G.; Lauceri, R.; Frish, L.; Evan-Salem, T.; Cohen, Y.; Zorzi, R. D.; Geremia, S.; Costanzo, L. D.; Randaccio, L.; Sciotto, D.; Purrello, R. *Chem.−Eur. J.* **2006**, *12* (10), 2722−2729; (c) Mammana, A.; D'Urso, A.; Lauceri, R.; Purrello, R. *J. Am. Chem. Soc.* **2007**, *129* (26), 8062−8063.
(39) Beller, C.; Bannwarth, W. *Helv. Chim. Acta* **2005**, *88* (1), 171−179.

tions per DNA strand. The porphyrin strands are generally very soluble in aqueous buffered solutions at pH 7 up to concentrations of 1 μM, which contrasts with our previously investigated tetranucleotide−diporphyrin arrays which are soluble in organic solvents only. The additional nucleotide units therefore dominate the solubility properties over the hydrophobic porphyrins. Interestingly, the electrophoretic mobility using denaturing PAGE shows that the porphyrin−DNA strands **5** and **6** tend to migrate slightly faster than the unmodified DNA (Figure 1). The bands become very streaky with increasing amount of modification, and more than three porphyrins prevent penetration of the strands into the gel.

Thermal denaturation measurements of the porphyrin−DNA duplexes (Table 1) reveal an average drop in melting temperature ΔT_m by 4.5 to 7 °C per porphyrin modification for strands **2** − **7**. Figure 2 displays the melting curves of the DNA duplexes. In the shorter strands, the increasing amount of porphyrin modification has a cumulative effect on the destabilization, but in the longer strands the destabilization effect is smaller. The ODN **8**, which contains 11 porphyrins, shows a melting temperature of 21.2 °C; here, the average decrease ΔT_m is 3.1 °C per porphyrin, which indicates a leveling off of the destabilization effect. This destabilization of the dsDNA is in the expected range for such a sterically rather demanding substituent.[13] In short strands (11-mer), the introduction of more than two porphyrins leads to duplexes that are not stable at ambient temperature. We have therefore concentrated on the 21-mer sequences for the spectroscopic analyses which show sufficient stability.

3. Structure of the Porphyrin−DNA

3.1. Double Stranded Porphyrin−DNA. The UV part of the CD spectra of the dsDNA **5•10** to **8•11**, which are displayed in Figure 3, shows the presence of a B-type DNA with a bisignate profile at −250/+276 nm, thus the porphyrin modification does not seem to distort the natural DNA structure to a very large extent. The duplex **8•11** with 11 porphyrins shows a reduced intensity of the CD signal at 250 nm from $\Delta\epsilon \approx -80$ M^{-1} cm^{-1} to $\Delta\epsilon = -35$ M^{-1} cm^{-1} but an increased signal intensity at 276 nm from $\Delta\epsilon \approx 60$ M^{-1} cm^{-1} to $\Delta\epsilon = 90$ M^{-1} cm^{-1}. In the porphyrin absorption region, an induced signal can be observed which is dominated by a negative signal at 422 nm. Some bisignate characteristics can be discerned in the spectra of the duplexes **5•10** and **8•11**. Normally, a negative induced signal indicates intercalation of the porphyrin within the base-stacking of the DNA.[40] This, however, is not a feasible alternative structure. First, the porphyrins are covalently attached to the nucleobase, and intercalation would have to be accompanied by base flipping of both the uridine and the adenosine of the complementary strand. Second, the acetylene-phenyl linker between the nucleobase and the porphyrin core

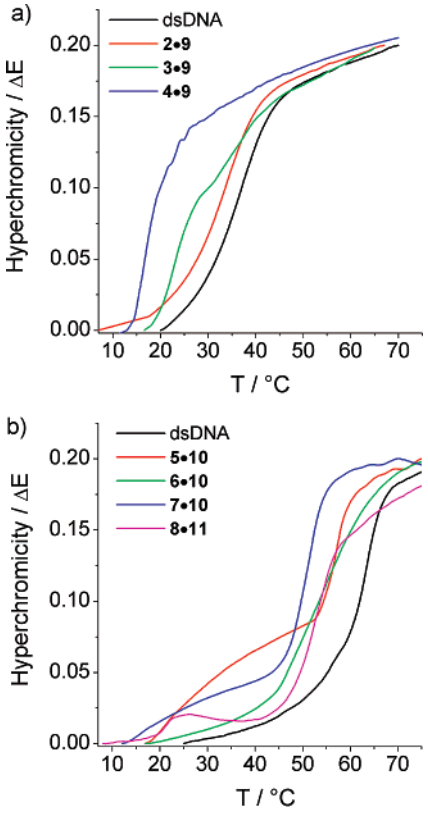

Figure 2. Thermal denaturing of the 11-mer (a) and 21-mer (b) porphyrin DNA duplexes (100 mM NaCl, 50 mM KH_2PO_4, pH 7.0, c(ODN) = 10^{-6} M).

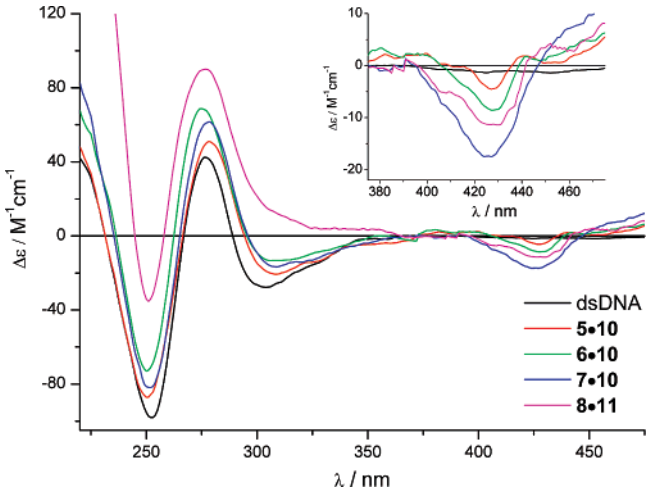

Figure 3. CD spectra of the double stranded porphyrin−DNA **5•10** to **8•11** (100 mM NaCl, 50 mM KH_2PO_4, pH 7.0, c(ODN) = 10^{-6} M).

is too long for the porphyrin to be placed in a position where stacking with the nucleobases could stabilize the structure; rather the porphyrin would protrude from the adjacent side of the double helix unless a severe distortion of the entire DNA structure occurred. This is also corroborated by structure calculations (see below). The negative Cotton effect can be explained by comparison with the spectra of the building block and the short tetranucleotide−diporphyrin arrays which we have investigated previously.[31] In **1**, the attachment of the chiral deoxyribose leads to a strong CD signal with a negative Cotton effect. This signal is independent of solvent (DCM, ethanol), metalation state (free base or zinc metalated), temperature (10

(40) (a) McMillin, D. R.; Shelton, A. H.; Bejune, S. A.; Fanwick, P. E.; Wall, R. K. *Coord. Chem. Rev.* **2005**, *249* (13−14), 1451−1459. (b) Bejune, S. A.; Shelton, A. H.; McMillin, D. R. *Inorg. Chem.* **2003**, *42* (25), 8465−8475. (c) Pasternack, R. F. **2003**, *15* (4), 329−332. (d) Pasternack, R. F.; Ewen, S.; Rao, A.; Meyer, A. S.; Freedman, M. A.; Collings, P. J.; Frey, S. L.; Ranen, M. C.; de Paula, J. C. *Inorg. Chim. Acta* **2001**, *317* (1−2), 59−71. Novy, J.; Urbanova, M.; Volka, K. *Vib. Spectrosc.* **2007**, *43* (1), 71−77. (e) Taima, H.; Okubo, A.; Yoshioka, N.; Inoue, H. *Chem.−Eur. J.* **2006**, *12* (24), 6331−6340. (f) Ghazaryan, A. A.; Dalyan, Y. B.; Haroutiunian, S. G.; Vardanyan, V. I.; Ghazaryan, R. K.; Chalikian, T. V. *J. Biomol. Struct. Dyn.* **2006**, *24* (1), 67−74. (g) Nitta, Y.; Kuroda, R. *Biopolymers* **2006**, *81*, (5), 376−391.

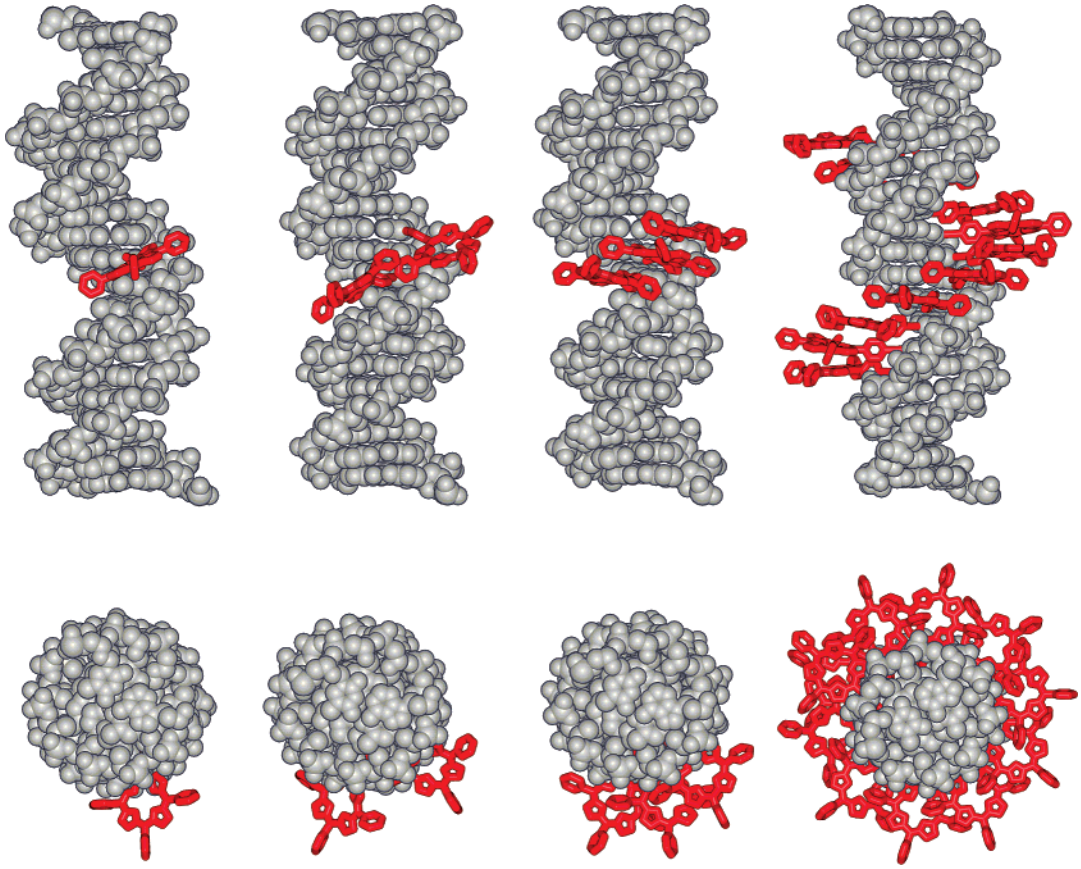

Figure 4. Side- and top-view of the force-field minimized structures of the duplexes **5•10**, **6•10**, **7•10**, and **8•11** (from left to right). Structures were obtained using the Macromodel software.[42]

to 80 °C), concentration (10^{-5} to 10^{-6} M), and potential ligands to the zinc in the porphyrin (up to 20% NEt_3); hence the porphyrin absorption is strongly perturbed by the nucleoside moiety. The covalent attachment of the porphyrin to the nucleotide renders the porphyrin itself chiral, thus the observed CD is an intrinsic not an induced CD. When **1** and other porphyrins are connected by a tetranucleotide scaffold, the negative Cotton effect persists.[31] Extending the DNA backbone from 4 to 21 nucleotides does not further alter the CD signal other than it broadens, as can be seen in the single strand arrays (see below). Upon duplex formation, the acetylene linker inhibits the chiral perturbation which the helical DNA should transfer to the porphyrin Soret band absorption. Even though the porphyrins interact which each other electronically (but not through exciton coupling), their electronic environment is overall dominated by a local perturbation induced by the chiral deoxyribose. Therefore, also in the porphyrin−DNA the CD signal associated with the porphyrin Soret band is intrinsic and not an induced signal, and we cannot draw conclusions of the sign of the CD, i.e., intercalation or outside stacking. In our case induced CD spectroscopy is not applicable for structure determination in the same way as compared to noncovalent DNA−porphyrin and DNA−drug interactions, or where the chromophore is attached to the DNA *via* sp^3-carbon containing linkers.[35,41]

The force-field minimized structures (AMBER)[42] of the porphyrin−DNA duplexes (Figure 4) show that the porphyrins are located in the major groove of the DNA with little overall perturbation of the DNA structure. In the duplexes **5•10** and **6•10**, the porphyrins are in-line with the groove at an averaged angle of 67° (porphyrin plane to DNA helical axis). The structure is reminiscent of a tetra-methyl pyridyl porphyrin DNA complex as determined by ^1H NMR spectroscopy.[43] If the porphyrins are adjacent to each other as in **7•10** and **8•11**, the porphyrins are aligned parallel to the base pairs. This is due to steric interactions between the phenyl substituents and the porphyrin core which restricts rotation around the acetylene linker and gives a more favorable structure overall when the porphyrins are stacked. The helicity of the dsDNA is only marginally distorted in the porphyrin region. The first and eleventh porphyrins in **8•11** are at a center-to-center distance of 3.37 nm and located directly above each other (Figure 4). However, since adjacent porphyrins are at a center-to-center distance of 0.91 nm, the overall length of the porphyrin array in **8•11** corresponds to a linear array of about 10 nm in length and spans a full helical turn in the dsDNA.

3.2. Single Stranded Porphyrin−DNA. The CD spectra of the single stranded porphyrin−DNA reveal that a significant amount of base stacking is preserved, because a bisignate signal was obtained in the UV part of the spectra (Figure 5a). The

(41) (a) Huang, X. F.; Nakanishi, K.; Berova, N. *Chirality* **2000**, *12* (4), 237−255. (b) Nehira, T.; Parish, C. A.; Jockusch, S.; Turro, N. J.; Nakanishi, K.; Berova, N. *J. Am. Chem. Soc.* **1999**, *121* (38), 8681−8691. (c) Balaz, M.; Bitsch-Jensen, K.; Mammana, A.; Ellestad, G. A.; Nakanishi, K.; Berova, N. *Pure Appl. Chem.* **2007**, *79*, (4), 801−809; (d) Berova, N.; Bari, L. D.; Pescitelli, G. *Chem. Soc. Rev.* **2007**, *36*, (6), 914−931.

(42) Mohamadi, F.; Richards, N. G. J.; Guida, W. C.; Liskamp, R.; Lipton, M.; Caufield, C.; Chang, G.; Hendrickson, T.; Still, W. C. *J. Comput. Chem.* **1990**, *11* (4), 440−467.

(43) Ohyama, T.; Mita, H.; Yamamoto, Y. *Biophys. Chem.* **2005**, *113* (1), 53−59.

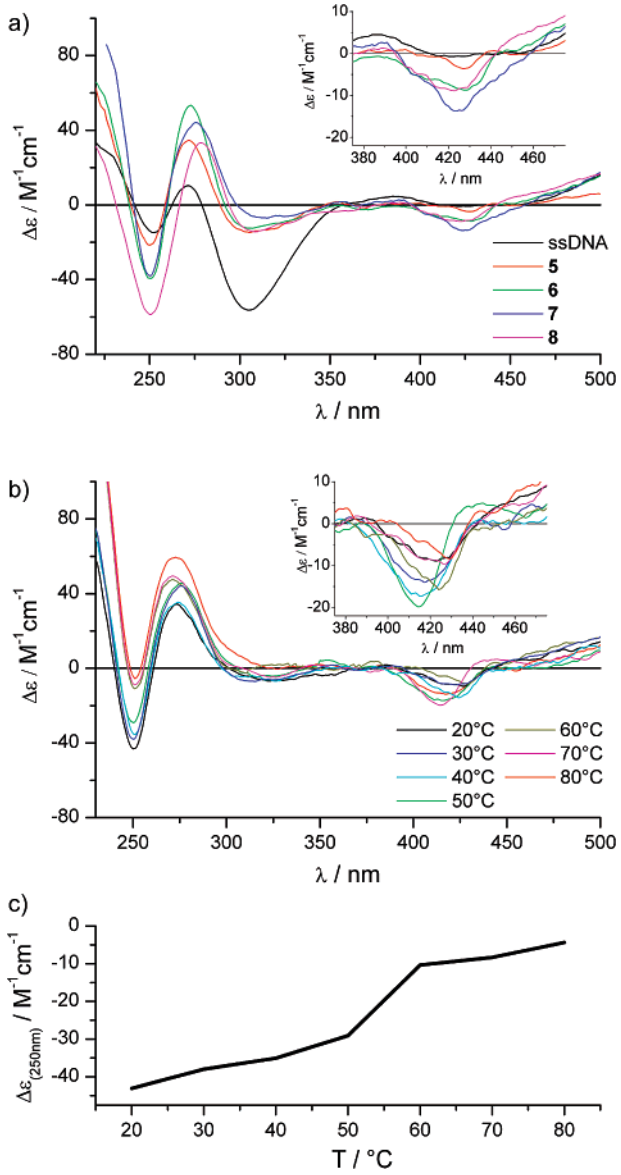

Figure 5. (a) CD spectra of the single stranded porphyrin-DNA **5** to **8** and unmodified DNA recorded at 20 °C. (b) *vt*-CD spectra of **7** from 20 to 80 °C. (c) $\Delta\epsilon$ vs T at 250 nm as obtained from the *vt*-CD spectra of **7**. All measurements were performed in 100 mM NaCl, 50 mM KH_2PO_4, pH 7.0, c(ODN) = 10^{-6} M.

unmodified DNA shows a negative signal at 300 nm, consistent with a random coil conformation. The signal intensities at −250/+276 nm are decreased compared to the DNA. In addition, a concomitant increase in the −250 nm signal can be seen with increasing amount of porphyrin modification. Again, the induced signals in the porphyrin absorption region are dominated by a negative peak at around 420 nm. The CD spectra indicate that in the single strand porphyrin−DNA, a helical structure is stabilized which seems to be induced by the porphyrin substituents. This is corroborated by the observation of a biphasic transition in the melting curve of the duplex **8•11** (Figure 2b), which has a first transition at 21.2 °C and a second larger transition at 52.3 °C, thus showing features of a two-stage melting process.

Also, variable temperature CD spectroscopy (*vt*-CD) of the single strands shows a transition upon heating, especially in the porphyrin absorption region. In Figure 5b, the *vt*-CD spectra of **7** are shown as a representative example. The spectra which show negative peaks at 427 nm at 20 °C transform to spectra with a more pronounced bisignate signal at 50 °C with peaks at (−420)/(+434) nm. Upon further heating, the signals re-broaden and shift to the red again with dominant negative peaks at 426 nm. An analogous observation was made when recording the *vt*-CD spectra of the duplexes. The porphyrin−DNA strands therefore undergo a structural change upon heating, where different conformations seem to dominate at ambient temperature and above 60 °C. A change is also observable in the DNA absorption region, and the profile of $\Delta\epsilon$ vs temperature indicates a transition between 50 and 60 °C. It is noteworthy that even at 80 °C a significant amount of residual helicity remains, and the porphyrin modified region does not seem to be fully denatured.

To obtain more information on the stability of this induced secondary structure, and also to address issues of possible aggregation or interstrand interactions, we performed various melting experiments with the single stranded porphyrin−DNA. The change in absorbance of the single strands at 260 nm was recorded, which is shown in Figure 6a for **5** to **8**. In the single porphyrin ODNs **2** and **5** no additional transition could be observed. For all other strands a transition is seen with reflection points at around 54 °C; the hyperchromicity corresponds well with the number of modified nucleobases. Since a temperature dependent change in absorbance is normally associated with unstacking of the nucleobases, this hyperchromicity is consistent with a change in structure and can be associated with an unwinding of an induced secondary structure in the single strands. If this structure stabilization is indeed induced by the porphyrins, then any structural changes might also have an influence on the electronic environment of the porphyrins. Changes in absorbance or fluorescence of DNA substituents upon thermal denaturing are generally observed and used in the analysis of DNA duplex stability.[17] As shown in Figure 6b, when recording the melting profiles of the single strands at 420 nm, where the porphyrins have their largest absorbance (*vide infra*), a transition can be observed as well. The reflection points of this transition (average 53.8 °C) correspond nicely to the ones measured at 260 nm (average 53.5 °C). Again, for the monoporphyrin strands **2** and **5** no transitions were detected.

Since the hydrophobic nature of the porphyrin could induce aggregation and thus formation of higher order oligomers, which might be responsible for the observed behavior of the single strands, thermal denaturing of the duplex **6•10** was measured at different concentrations (Figure 6c) from 10 to 55 nM, where a significant change in the duplex melting temperature is expected.[44] In this case, the melting profiles were recorded using the decrease of the emission maximum of the porphyrins at 640 nm (excitation at 420 nm) upon denaturing of the duplex. The melting curves show biphasic transitions, where the first transition is strongly dependent on the concentration and varies from 48.8 °C at 55 nM to 40.5 °C at 10 nM concentration. The second transition is independent of concentration and has a melting temperature of ∼54 °C (T_p in Figure 6c). The two transitions are not very prominent in the melting profiles but are clearly visible in the first derivative of the curves as shown in Figure 6d. The second transition which leads to an additional

(44) Davis, T. M.; McFail-Isom, L.; Keane, E.; Williams, L. D. *Biochemistry* **1998**, *37* (19), 6975−6978.

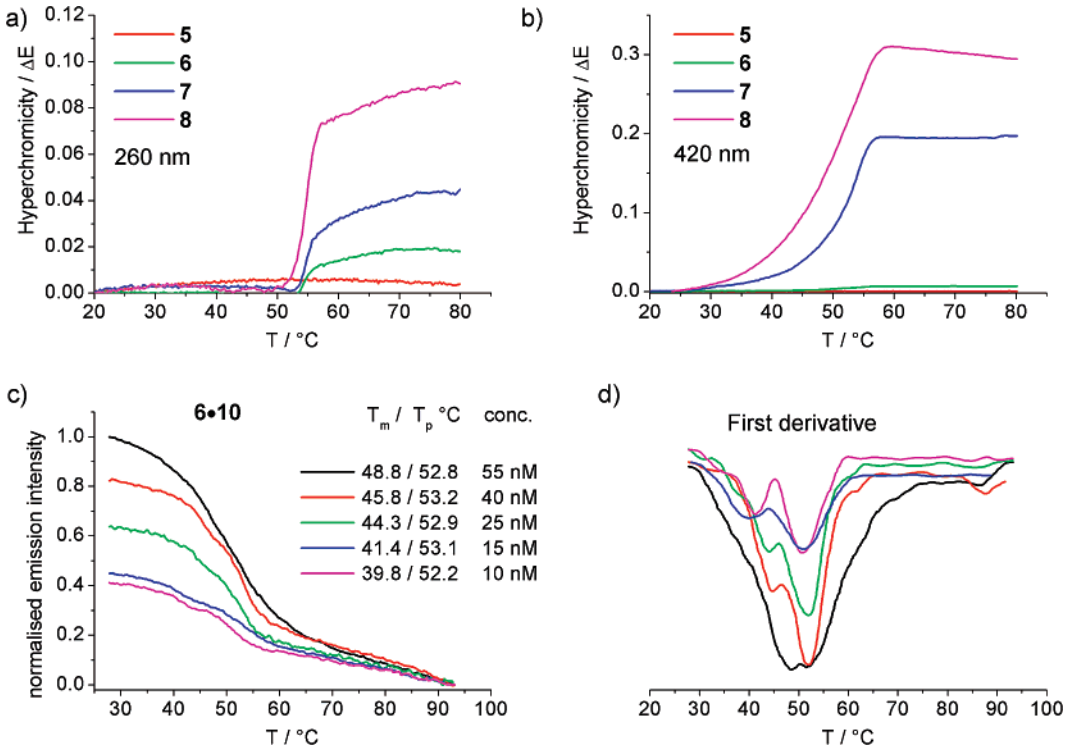

Figure 6. Top: phase transition of the single-strand porphyrin DNA recorded using the change in UV−vis absorbance at (a) 260 nm and at (b) 420 nm (100 mM NaCl, 50 mM KH_2PO_4, pH 7.0, c(ODN) = 10^{-6} M); bottom: (c) concentration dependent melting of the duplex **6•10** using the emission of the porphyrin at λ = 640 nm (excitation at λ = 420 nm), (d) first derivatives of the melting curves of (c).

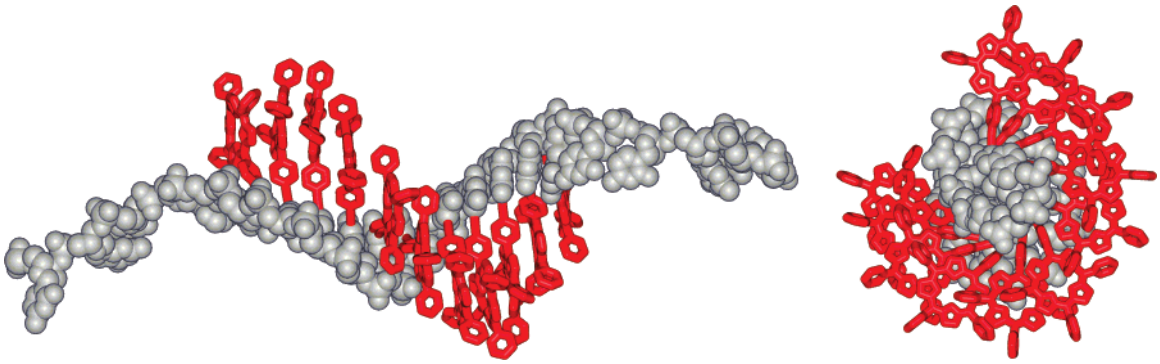

Figure 7. Side- and top-view of the force-field minimized structure of **8**. The structures were obtained using the Macromodel software[42] starting from a random conformation of the porphyrin−DNA.

hyperchromicity in both the DNA and porphyrin absorbance is therefore due to a concentration independent intramolecular event and not associated with disruption of higher order structures arising from interstrand interactions.[44] Similar biphasic transitions were also observed for the melting of hairpin structures.[45] For the single stranded porphyrin−DNA, we have also performed force-field structure minimization starting from a random conformation, and the porphyrin modified region indeed shows a helical stacked arrangement as a minimum energy conformation, whereas the unmodified part of the DNA tends to adopt a random-coil structure. Figure 7 displays the conformation of **8** which was obtained from the minimization. Also in **6** and **7**, the porphyrins can approach closely enough to form stacked dimer and trimer structures, respectively, which is consistent with the change in both absorption and emission spectra upon hybridization (*vide infra*) and with the residual helicity observed in the CD spectra. In **8**, the minimized structure shows an α-helical conformation which is elongated compared to the duplex DNA. The center-to-center distance between the first and last porphyrin is at 4.15 nm, which is 0.78 nm further than that in **8•11**, and the porphyrins are more closely packed than in the double strand. Induced preorganization is known for propynyl modified poly-dU,[46] but with the porphyrin substitution a much larger stabilization is observed.

In a nondenaturing PAGE experiment, the stability of the secondary structures in **7** and **8** becomes visible when the gels are run at different temperatures. At 10 °C, **7** migrates as a much narrower band as in the denaturing gel (Figure 8, lane a), but the band is still larger than what can be observed for unmodified DNA. At 60 °C, the band becomes very streaky and is identical to the migration pattern in denaturing PAGE. At low temperature, **8** does not migrate at all (lane b) except for when the

(45) Trafelet, H.; Parel, S. P.; Leumann, C. J. *Helv. Chim. Acta* **2003**, *86* (11), 3671−3687.

(46) Znosko, B. M.; Barnes, T. W.; Krugh, T. R.; Turner, D. H. *J. Am. Chem. Soc.* **2003**, *125* (20), 6090−6097.

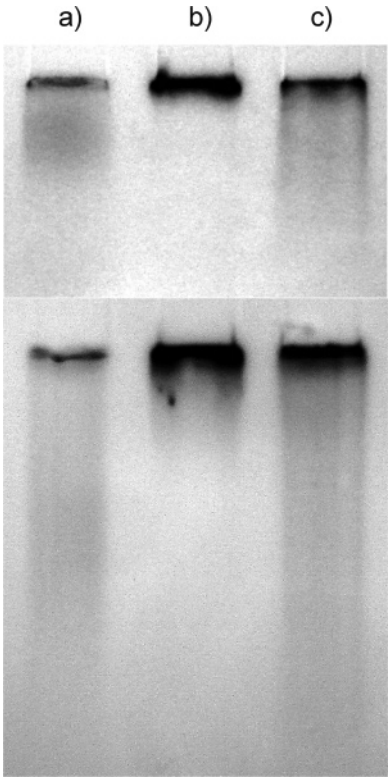

Figure 8. Native PAGE of **7** (lane a), **8** (lane b), and **8** pretreated with 1 M urea in DMF (lane c). The gels were run at 10 °C (top) and 60 °C (bottom) for 2.5 h at constant voltage (200 V).

DNA is pretreated with urea and DMF to induce denaturing of the secondary structure (lane c). In this case a short smeary band can be observed with most of the DNA remaining in the very first part of the gel. When the temperature is raised to 60 °C, the strand **8** starts to migrate, visible in the smearing below the start point of the gel. Pretreatment of **8** with urea and DMF again shows enhanced migration and smearing across a large part of the gel. At higher temperature the modified DNA therefore has an increased flexibility due to partial denaturing of the secondary structure; the effect is larger when using urea and DMF as active denaturing agents.

4. Absorption and Emission Spectroscopy

It should be noted that the length and the sequence of the DNA scaffold does not influence the electronic properties of the porphyrin. We therefore concentrated on the 21-mer system which shows enhanced stability as duplexes at ambient temperature. There are basically three different conditions that have to be investigated based on the impact of complementary strand and temperature on the preferred conformation of the porphyrin−DNA, namely (i) single strands and (ii) double strands at ambient temperature (i.e., 15 °C) and (iii) porphyrin−DNA at high temperature (i.e., 80 °C). Figure 9 shows the absorbance spectra of the single strands **5** to **8** and the double stranded porphyrin−DNA **5•10**, **6•10**, **7•10**, and **8•11**, both at 15 and 80 °C. The extinction coefficients show alteration upon hybridization with the complementary strand (Table 2); therefore the placement of the porphyrin in the major groove of the double helix has quite a significant influence on the electronic environment of the chromophore. However, the changes in **2** and **5** are only marginal. The single porphyrin DNA strand has an absorption spectrum reminiscent of a porphyrin in organic solvent. The water soluble building block $dU^{2HTCTPP}$, which contains three carboxylic acid groups on the *meso*-phenyl substituents, shows a B-band absorption maximum at $\lambda_{max} = 414$ nm ($\log \epsilon = 5.44$),[29] whereas in organic solvents the free base tetraphenyl substituted deoxy uridine dU^{2HTPP} has a maximum at $\lambda_{max} = 420$ nm ($\log \epsilon = 5.62$), which is due to the different solvent polarity of $CHCl_3$ versus H_2O.[9] In **5**, we find an absorption maximum of the porphyrin B-band at $\lambda = 422$ nm ($\log \epsilon = 5.35$). The λ_{max} shows that the porphyrin is in a rather hydrophobic environment, which is consistent with the more hydrophobic nature of the major groove of the duplex DNA.[47] However, polarity differences to pure $CHCl_3$ are evident because of the hypochromicity of ~40% of **5** compared to dU^{2HTPP}.

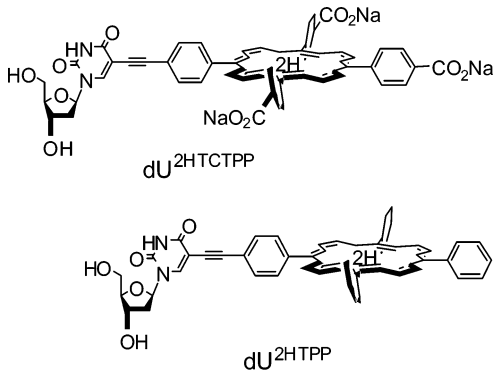

In the two and three porphyrin arrays **6** and **7**, the extinction coefficients of the B-bands increase compared to **5** as expected. A substantial broadening is observed, even when the two porphyrins are separated by a nonmodified thymidine, and a shoulder at lower wavelength becomes apparent. In the 11 porphyrin array, the extinction coefficient is much lower than would be expected from a superposition of the absorbance of 11 porphyrins. The porphyrin absorption band also appears very broad. In all multiporphyrin arrays, the B-band absorption can be deconvoluted into two absorption bands with maxima at 404 to 409 nm and at 422 to 439 nm with variable intensities (Figure 9e). A clear indication of electronic interactions between the porphyrins is given, though this may not be very strong because the B-bands are not split into two distinct absorbances. Analogous observations are usually made in stacked porphyrin arrays; therefore the DNA backbone provides a scaffold for arranging the porphyrins into ordered stacks, confirming the structures as obtained from the calculations. The same broadening of the B-band absorbance can be observed in the double stranded forms.

At high temperature (80 °C), both single and double stranded porphyrin−DNA exhibit identical absorbance, which confirms complete denaturing of the duplexes. Again, a major difference to the room temperature absorbance is observed in the multiporphyrin systems, which can be explained by a change in overall structure of the porphyrin arrays. Generally, the porphyrin B-bands become sharper with an increase in log(ϵ) of 13%, 92%, and 60% for **6**, **7**, and **8**, respectively. This is consistent with the unstacking of the porphyrins at high temperature, but for **8** there may still be stacked regions

(47) Privalov, P. L.; Dragan, A. I.; Crane-Robinson, C.; Breslauer, K. J.; Remeta, D. P.; Minetti, C. *J. Mol. Biol.* **2007**, *365* (1), 1−9.

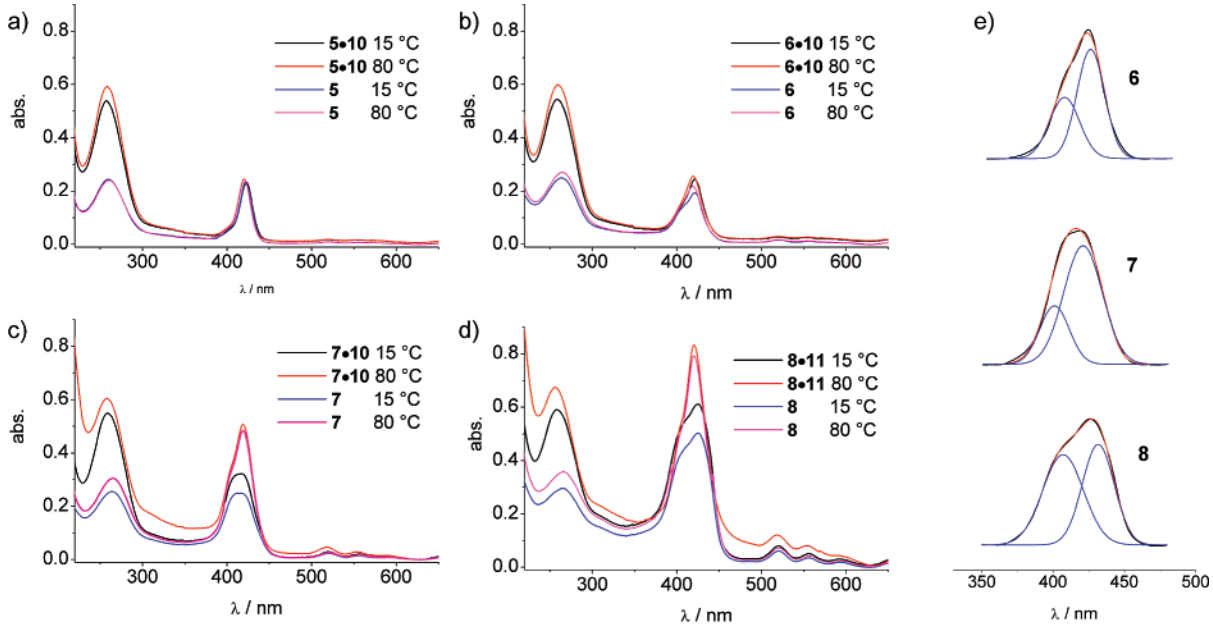

Figure 9. (a to d) UV−vis absorbances of the single and double stranded porphyrin−DNA; (e) *Gaussian* deconvolution (blue lines) of the B-band absorption region of the single strand porphyrin−DNA (15 °C, black lines), the red lines are the calculated spectra based on the *Gaussian* deconvolution. 100 mM NaCl, 50 mM KH_2PO_4, pH 7.0, c(ODN) = 10^{-6} M.

Table 2. Absorption and Emission Data of the ODN Strands **2** to **8** as Single and Double Strands

	absorption maxima/nm (log ϵ)			emission maxima/nm (rel. Int.)
5	260 (5.38)	422 (5.35)	521 (4.26), 554 (4.24), 583 (4.13), 648 (3.53)	652 (0.46), 715 (0.10)
5•10	260 (5.73)	420 (5.39)	521 (4.27), 557 (4.25), 583 (4.14), 647 (3.54)	652 (0.70), 714 (0.15)
6	260 (5.39)	403 (sh), 421 (5.28)	519 (4.24), 557 (4.12), 590 (3.90), 653 (3.78)	656 (0.73), 718 (0.19)
6•10	260 (5.74)	408 (sh), 421 (5.39)	519 (4.23), 554 (4.13), 584 (3.92), 652 (3.79)	653 (1.00), 716 (0.23)
7	260 (5.41)	415 (5.39)	520 (4.42), 557 (4.21), 590 (4.18), 650 (3.87)	654 (0.24), 718 (0.06)
7•10	260 (5.74)	415 (5.51)	520 (4.43), 556 (4.22), 590 (4.19), 650 (3.89)	656 (0.34), 717 (0.08)
8	262 (5.74)	406 (sh), 425 (5.70)	520 (4.85), 556 (4.62), 594 (4.37), 652 (4.26)	657 (0.05), 720 (0.01)
8•11	262 (5.77)	406 (sh), 424 (5.78)	520 (4.86), 556 (4.63), 594 (4.38), 652 (4.27)	656 (0.07), 719 (0.02)

in the array because the hyperchromicity is much less pronounced as would be expected when compared to **7**. Also in the UV part of the absorption spectra, i.e., in the DNA region, a hyperchromicity can be seen as would be predicted from the melting curves. The observations are very well in line with the melting curves and the structure calculations.

The emission spectra further confirm the presence of a stacked array because a strong quenching is observed when two or more porphyrins are adjacent to each other as in **7** and **8** (Figure 10, Table 2). In **6•10**, the two porphyrins are not stacked, and the luminescence intensity increases compared to **5•10**. Some quenching still occurs because the luminescence intensity of **6•10** is not double that of **5•10**. Upon hybridization, a large increase in luminescence is consistent with placing the porphyrins in a less solvated environment, and the effect is largest in **5** and smallest in **8**. In **5**, the single porphyrin seems to be strongly solvated, and placement in the major groove has a large impact on the electronic environment. This is consistent with reports on the change of fluorescence of 5-alkynyl deoxyuridines upon hybridization[48] and was attributed to differences in solvation.[49] Since the multiporphyrin arrays are stacked in the single strands, which already desolvates most of the porphyrins, the impact on environmental changes caused by hybridization is less pronounced. Recording the spectra at 80 °C reveals a further decrease in the luminescence intensity, which is presumably a combination of unstacking of the porphyrins together with a much stronger solvation in an aqueous environment. The luminescence of porphyrins is normally decreased in aqueous solvents compared to organic solvents, but unstacking would lead to an increase of luminescence intensity. Therefore, the solvation of the porphyrins upon unstacking seems to dominate the electronic properties of the excited state. The decrease in luminescence intensity upon denaturing of the systems leads to the melting curves as shown in Figure 6c. Changes in the

(48) Xiao, Q.; Ranasinghe, R. T.; Tang, A. M. P.; Brown, T. *Tetrahedron* **2007**, *63* (17), 3483−3490.
(49) Hudson, R. H. E.; Ghorbani-Choghamarani, A. *Org. Biomol. Chem.* **2007**, *5* (12), 1845−1848.

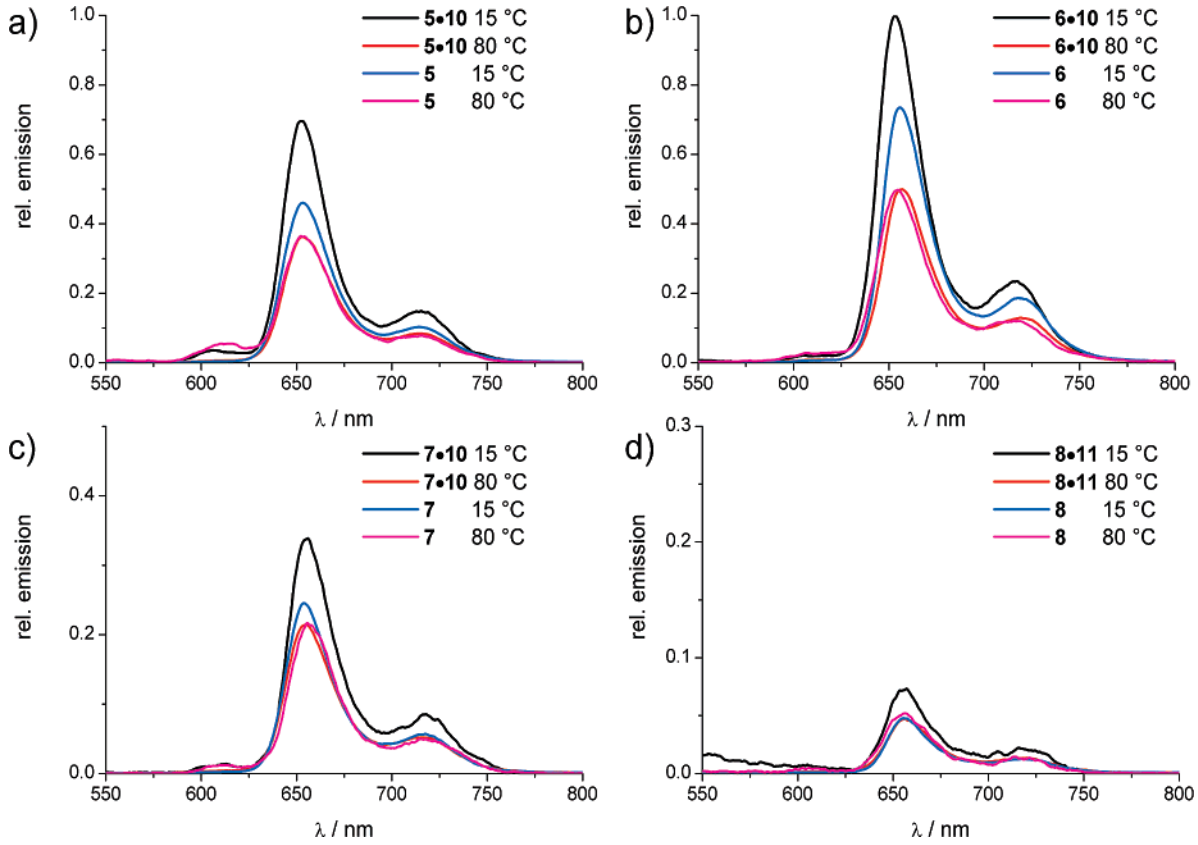

Figure 10. Steady-state emission spectra of the porphyrin−DNA as single and double strands, at 15 and 80 °C. 100 mM NaCl, 50 mM KH_2PO_4, pH 7.0, c(ODN) = 10^{-7} M.

wavelengths of the emission maxima are only marginal, and no degradation of the chromophore was observed upon up to 5 h of continuous illumination.

5. Conclusions

We have shown that porphyrin substituted deoxy-uridine provides a versatile building block for the synthesis of porphyrin arrays on the nanometer scale. The porphyrins can be introduced site specifically into the DNA strands, and the electronic properties of the array can thus be tuned. If the porphyrins are separated by an unmodified nucleotide, the ground state is affected to some extent, and the luminescence increases with increasing amount of porphyrins. On the other hand, adjacent porphyrins have a strong tendency to stack even in the single strand leading to an ordered structure, and both ground state and excited state are influenced by the neighboring porphyrin. However, the electronic interactions in the ground state are not very strong, because the porphyrin B-band absorptions are not split into two well separated absorbances. The porphyrin−DNA exhibits an induced secondary structure in the single strands, which is stable up to ~54 °C. The α-helical structure of the single stranded array is comparable to B-type DNA but in a more extended form, where the porphyrins can stack more efficiently than in the duplex form. Upon hybridization, the porphyrins are placed in the major groove of the DNA leading to desolvation and a slightly larger porphyrin-to-porphyrin distance. This is expressed in an increase in absorbance and luminescence intensity; this effect, however, depends strongly on the sequence of the porphyrin array. The melting experiments, absorbance and emission measurements, and structure

Scheme 2. Schematic Representation of the Two-Stage Melting Process in the Porphyrin−DNA Arrays

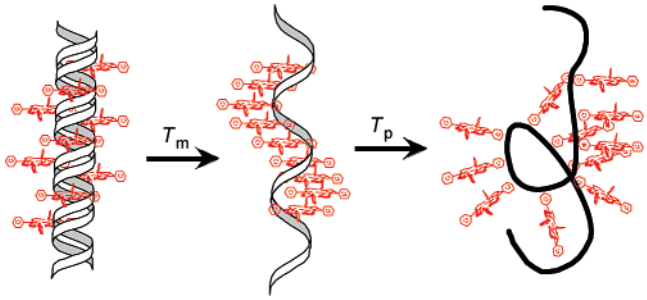

calculations are all consistent with both the double helical structure of the porphyrin−DNA and the induced secondary structure in the single strands. Depending on the length of the ODN and the amount of porphyrins, a two-stage melting process can be observed with $T_m \neq T_p$ (Figure 6, Scheme 2), where T_m is the melting temperature of the duplex, and T_p is the unwinding temperature of the single stranded porphyrin system. Noteworthy T_p is independent of the amount and sequence of the porphyrin modification.

From a synthetic point of view, it seems that there is no limitation in the amount of incorporated chromophores, and this system is therefore very attractive to create long arrays by an automated synthesis. Furthermore, the sequence of the array can be tuned simply by reprogramming the DNA synthesizer. The duplex stability decreases with increasing amount of porphyrin modification as could be expected, and a flanking sequence of a certain length is necessary to maintain duplex stability in the multiporphyrin arrays. However, since the single-stranded

porphyrin−DNA orders itself into a stacked α-helical conformation, it seems that this is a very convenient way of synthesizing an ordered nanometer-long porphyrin array, and the complementary strand is in principle not required to maintain order. The only comparable system to date is pyrene−RNA or −DNA, and in none of these arrays have similar observations been made. It therefore requires a larger aromatic system than pyrene to induce stable stacks, which can be achieved with porphyrins. This structure stabilization is independent of the amount of porphyrins and is quite unexpected. It appears that the porphyrins interact more strongly in the single-strand than in the double-strand, which leads to a low T_m and a high T_p. The more efficient stacking of the porphyrins becomes apparent in the minimized structures. It will certainly be interesting to see where the limits are to which large groups can be arranged on either single- or double-stranded DNA. The systems are currently being evaluated for their ability to function as photonic or electronic wires, and more studies regarding emission spectroscopy (i.e., excited-state lifetimes and energy transfer processes) are under way, especially in combination with other chromophores.

Acknowledgment. Financial support from the Swiss National Science Foundation (Grant No. 200020-107703), the EPSRC (Grant No. EP/E045693/1), and the Treubel Foundation Basel (Fellowship to E.S.) is gratefully acknowledged. We thank Prof. Nina Berova (Columbia University) and Dr. Giuliano Siligardi (Diamond Light Source Ltd, U.K.) for helpful discussions on CD spectroscopy and ATDBio (Southampton, U.K.) for generous support in DNA synthesis and analysis.

Supporting Information Available: Synthetic protocols for the porphyrin−DNA and purification of the porphyrin−DNA strands, force-field minimized structures of **5** and **6**. Complete ref 1b. This material is available free of charge via the Internet at http://pubs.acs.org.

JA075711C